

# Electrical and Thermal Magnetoconductivities of Single-Crystal Beryllium at Low Temperatures and Its Use as a Heat Switch\*

Ray Radebaugh

Cryogenics Division, Institute for Basic Standards,  
National Bureau of Standards, Boulder, Colorado

(Received September 24, 1976)

*The effects of transverse magnetic fields up to 955 kA/m (12 kOe) on the electrical and thermal conductivities of single-crystal beryllium have been measured between 2 and 300 K. Most of the measurements were made on a sample with a resistance ratio of 1340. This sample was pure enough so that the intrinsic electronic thermal resistivity could be measured for the first time. It was found to have the usual  $T^2$  behavior. The current and heat flow were along the hexagonal c axis of the crystal, while the thermal and electrical conductivities were studied as a function of the angle of the magnetic field in the basal plane. Below about 50 K the thermal conductivity could be reduced by several orders of magnitude by applying the magnetic field. The lattice conductivity, extrapolated from the measurements in the magnetic field, is given by  $k = \gamma T^2$ , where  $\gamma = 1.6 \times 10^{-4} \text{ W/cm K}^3$ . This value is in reasonable agreement with that obtained from measurements of beryllium alloys. The use of single-crystal beryllium as a heat switch for temperatures below about 30 K is discussed.*

## 1. INTRODUCTION

Heat is conducted in a metal by lattice waves,  $k_l$ , as well as by electrons,  $k_e$ , so that the total thermal conductivity is given by  $k = k_l + k_e$ . For high-purity metals  $k_e$  completely dominates  $k_l$  at low temperatures. However, the application of a transverse magnetic field can decrease  $k_e$  to the point where most of the heat is conducted by the lattice waves. The lattice thermal conductivity, which is independent of magnetic field, can then be measured easily. Because of the high Debye temperature of beryllium,  $k_l$  is expected to be lower than for any other metal and  $k_e$  should become large at a

\*This research was supported by the Advanced Research Projects Agency of the Department of Defense and was monitored by ONR under Government Order Number NAonr-1-75.

relatively high temperature. The application of a transverse magnetic field then should change the total thermal conductivity by several orders of magnitude. The relatively high electrical magnetoresistive effect in beryllium<sup>1</sup> means that modest fields could cause such a change in thermal conductivity. Beryllium then appears to be an excellent choice for use as a heat switch at low temperatures. In the past gallium has been used as a magnetothermal heat switch,<sup>2</sup> and magnetothermal conductivity data on tungsten<sup>3,4</sup> indicate that it, too, would be a good material for a heat switch. Both gallium and tungsten can operate as heat switches up to about 10 K. The high Debye temperature of beryllium suggests that it may be a useful switch at temperatures even above 10 K.

The only previous magnetothermal conductivity measurements of high-purity beryllium were those of Grüneisen and co-workers.<sup>5-7</sup> Their best sample had a residual resistivity ratio (RRR)  $\rho_{295}/\rho_4$  of 948. Though their measurements were made at only 23.5 and 81 K, the data do indicate that beryllium could be a good heat switch. In order to clarify the situation, more measurements of the magnetothermal conductivity of high-purity beryllium at low temperatures were needed. In addition, the existing data<sup>8</sup> on the thermal conductivity of beryllium in zero field between 90 and 300 K were for a rather impure sample. Those results were not consistent with that of Grüneisen<sup>5-7</sup> below 90 K, nor with the extensive data above 300 K by Powell.<sup>9</sup> For that reason the present measurements were made over the whole region between 2 and 300 K.

## 2. EXPERIMENTAL METHOD

### 2.1. Samples

The work of Grüneisen<sup>5-7</sup> showed that the maximum field effect occurred with the heat flow along the hexagonal  $c$  axis and the magnetic field in the basal plane along an  $a$  axis such as  $\langle 11\bar{2}0 \rangle$ . For this reason the samples obtained for this work had the long axis of the crystal along the hexagonal  $c$  axis. Two different single-crystal samples were measured. Most of the measurements were made on a very high-purity sample, which will be denoted as sample 1. This sample was loaned to us by Dr. R. J. Soulen of the Heat Division of the National Bureau of Standards. He in turn received the sample from Dr. W. Reed of Bell Telephone Laboratories. That sample was one of several that Dr. Reed cut out from a much larger single crystal grown by Nuclear Metals, Inc. The size of the crystal we received was 3 mm  $\times$  3 mm  $\times$  25 mm. The hexagonal  $c$  axis was along the long axis of the crystal to within 1° as determined from back-scattered x-ray Laue photographs. The

residual resistivity ratio  $\rho_{295}/\rho_4$  was measured by a potentiometric technique and found to be 1340.

Sample 2 was spark-cut from a single-crystal disk piece given to us by Dr. S. K. Sinha of Iowa State University. This sample was  $2.3 \text{ mm} \times 3.7 \text{ mm} \times 16 \text{ mm}$  with the  $c$  axis within  $2^\circ$  of the long axis of the crystal. The resistivity ratio  $\rho_{295}/\rho_4$  was found to be 79. After the sample was spark-cut, it was etched in a solution with composition 26.5 ml conc.  $\text{H}_2\text{SO}_4$ , 450 ml conc.  $\text{H}_3\text{PO}_4$ , 53 g  $\text{CrO}_3$ , held at a temperature of about  $70^\circ\text{C}$ . The ends of this etched sample were then tinned with 99.99% pure indium, using an ultrasonic soldering iron and zinc chloride flux.

## 2.2. Experimental Techniques

The thermal conductivities of the two beryllium samples were measured by using the standard technique of observing the temperature drop across a portion of the sample while a steady heat current flowed through the sample. A schematic of the apparatus is shown in Fig. 1. Carbon thermometers of 1/8 W size and  $220 \Omega$  normal resistance with a flat ground on one side were used as temperature sensors. Two thermometers were varnished to the sample to measure the  $\Delta T$  across the sample and one thermometer was mounted on the reservoir close to the sample. The reservoir thermometer then allowed measurements of the thermal resistance at the boundary between the sample and the reservoir. A constant-current source and a digital voltmeter were used to read the carbon thermometers. A germanium

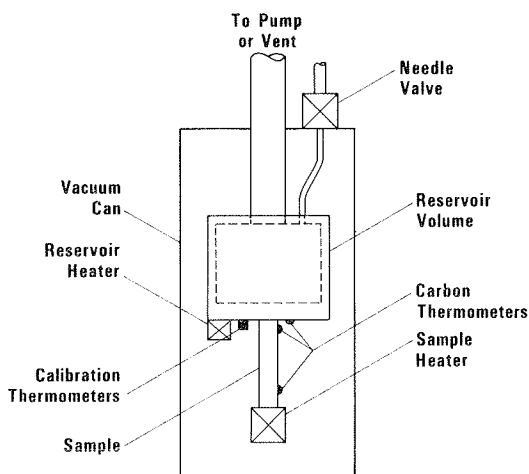


Fig. 1. Schematic diagram of apparatus used to measure the thermal conductivity of beryllium.

thermometer, calibrated by the manufacturer, was also mounted on the reservoir to calibrate the three carbon thermometers. A capacitance thermometer,<sup>10</sup> also mounted on the reservoir, served to calibrate the other thermometers in a magnetic field. The magnetoresistance of the carbon thermometers agreed with previously published results<sup>11</sup> in the temperature range 1.8–18 K. Magnetoresistance corrections above 18 K are negligible for fields used in this work. For measurements between 100 and 300 K thermocouples of KP versus Au–0.07% Fe were used for measurements of both  $T$  and  $\Delta T$ . Published thermocouple tables<sup>12</sup> were used to convert voltages to temperatures. Magnetic field corrections are negligible in this temperature range.

An aluminum foil radiation shield (not shown in Fig. 1) surrounded the sample and was attached to the reservoir. The reservoir, made entirely of copper, was a 10-cm<sup>3</sup> pot suspended inside the vacuum can by a 6-mm-diameter, stainless steel pumping tube. Liquid nitrogen or liquid helium outside the vacuum can could be let into the reservoir through a stainless steel capillary tube with a valve in the liquid bath. With such an arrangement the reservoir could be cooled to the bath temperature within a few minutes by opening the valve in the liquid bath while the pumping tube on the reservoir was vented to the atmosphere. Measurements below the bath temperature were made by closing the needle valve and pumping on the reservoir. Measurements above the bath temperature were made by first closing the needle valve and applying current to the reservoir heater to boil off the liquid in the reservoir. When the temperature rose to the desired point the needle valve was opened just enough to provide a cooling effect to nearly balance the heat input to the reservoir. The carbon thermometers were calibrated during that procedure. Next the power to the reservoir heater was turned off as the same power was applied to the sample heater for measurement of the thermal conductivity. This procedure gave rather rapid equilibrium times and usually yielded very stable temperatures.

The reservoir and vacuum can were made small in diameter so as to fit in the tails of nested glass dewars. These tails, in turn, were fit between the poles of an iron core electromagnetic which could attain a field of 955 kA/m (12 kOe).

The high-purity sample 1 was thermally anchored to the reservoir with a low-temperature varnish. That sample was to be used later for superconducting fixed point measurements and contamination with solder was not desirable. The heater was attached to the other end of the sample with varnish also. The thermal boundary resistance of the varnish joint was on the order of 20 K/W, which was much higher than the 0.2 K/W thermal resistance of the sample in zero field at low temperatures. Thus, accurate measurements in zero field were difficult to make because of the necessity

for low power levels to keep the entire sample from heating too much. Heat leaks out through the electrical leads amounted to only about 0.1% of the total power input to the sample.

Sample 2 was tinned with pure indium on each end as described previously. One end of this sample was then indium-soldered to the reservoir and the heater mounting bracket soldered to the other end. The indium solder provided much better thermal contact for this sample.

The electrical conductivities of both beryllium samples were measured potentiometrically. Current and voltage leads were pressure contacts to the sample. Pointed brass screws were used for the voltage taps and the distance between the indentions was measured with a traveling microscope. Currents up to 2 A were used when the sample conductivity was high. The same thermometers used for the thermal conductivity measurements were used to determine the sample temperature during the electrical conductivity measurements. The rather large-diameter current leads necessary to measure the electrical conductivity precluded the measurement of electrical and thermal conductivities during the same cooldown.

### 3. EXPERIMENTAL RESULTS

The temperature dependence of the electrical resistivity of sample 1 is shown in Fig. 2. These data are for the current along the hexagonal  $c$  axis [0001] and the magnetic field along the  $a$  axis. Results of previous measurements<sup>5,9,13</sup> in zero field on less pure samples are also shown for comparison. The total resistivity is conventionally expressed as

$$\rho_t = \rho_i + \rho_r \quad (1)$$

where  $\rho_i$  is the intrinsic resistivity due to scattering of electrons by phonons and  $\rho_r$  is the residual resistivity due to impurity scattering of the electrons. For sample 1 we have  $\rho_r = 3.35 \times 10^{-3} \mu\Omega\text{-cm}$  and  $\rho_i = 1.0 \times 10^{-9} T^4 \mu\Omega\text{-cm}$ . This expression for  $\rho_i$  is identical with that found by Reich *et al.*<sup>13</sup> on a less pure sample. For our sample we find  $\rho_{0^\circ\text{C}} = 3.69 \mu\Omega\text{-cm}$  and  $\rho_{23^\circ\text{C}} = 4.48 \mu\Omega\text{-cm}$ . These data are in good agreement with the value  $\rho_{0^\circ\text{C}} = 3.58 \mu\Omega\text{-cm}$  found by Grüneisen and Adenstedt.<sup>5</sup> Our measured values for  $\rho$  have an inaccuracy of about 5%, which arises mainly from geometric uncertainties. The variation of the resistivity with the angle of the magnetic field in the basal plane is shown in Fig. 3 for a temperature of 4 K and in Fig. 4 for a temperature of 76 K. In both cases the magnetic field was 796 kA/m (10 kOe). These curves show the 60° rotational symmetry expected for a hexagonal crystal.

Figure 5 shows the thermal conductivity of sample 1 as a function of temperature for several magnetic fields. The heat flow was along the

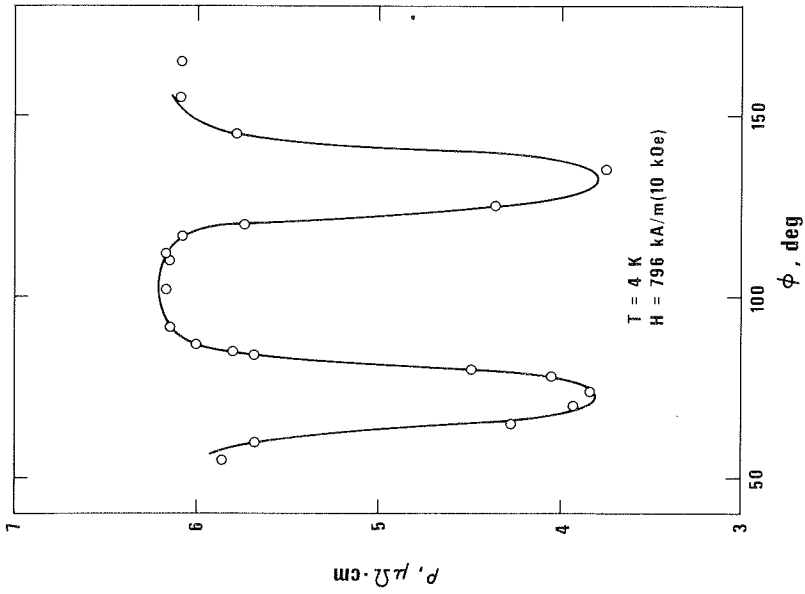


Fig. 3. The electrical resistivity of high-purity single-crystal beryllium at 4 K as a transverse magnetic field of 796 kA/m (10 kOe) is rotated about the basal plane. The angle  $\phi$  is an arbitrary angle.

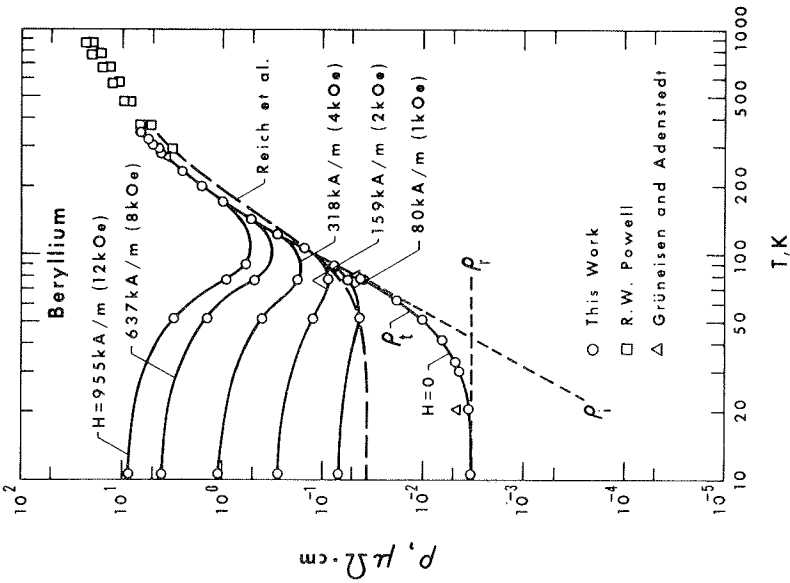


Fig. 2. The electrical resistivity of high-purity single-crystal beryllium as a function of temperature in various transverse magnetic fields. Previous results from Refs. 5, 9, and 13 on less pure samples are shown for comparison.

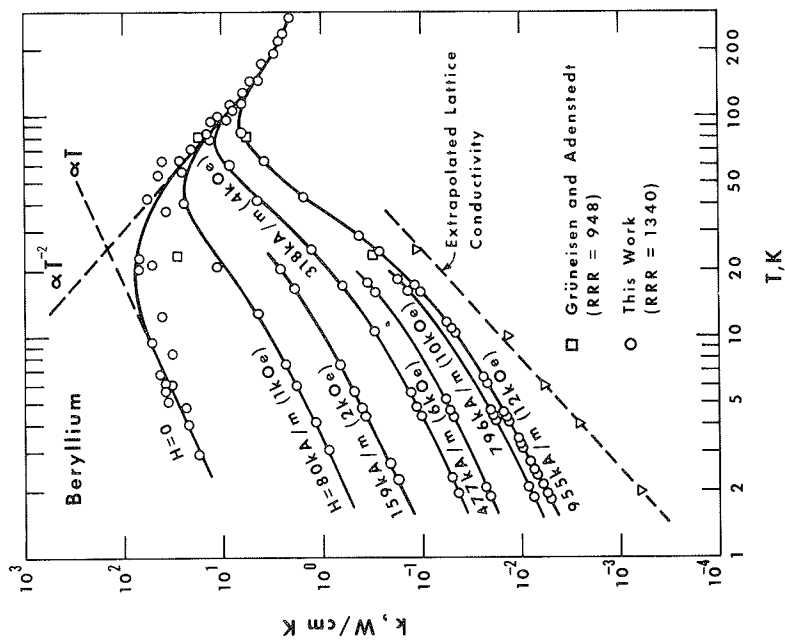


Fig. 5. The thermal conductivity of high-purity single-crystal beryllium as a function of temperature for various transverse magnetic fields. The work of Grüneisen and Adenstedt from Ref. 5 is shown for comparison. Their points are for magnetic fields of 0 and 955 kA/m (12 kOe). The triangles represent points where the lattice conductivity was derived from extrapolations in finite fields.

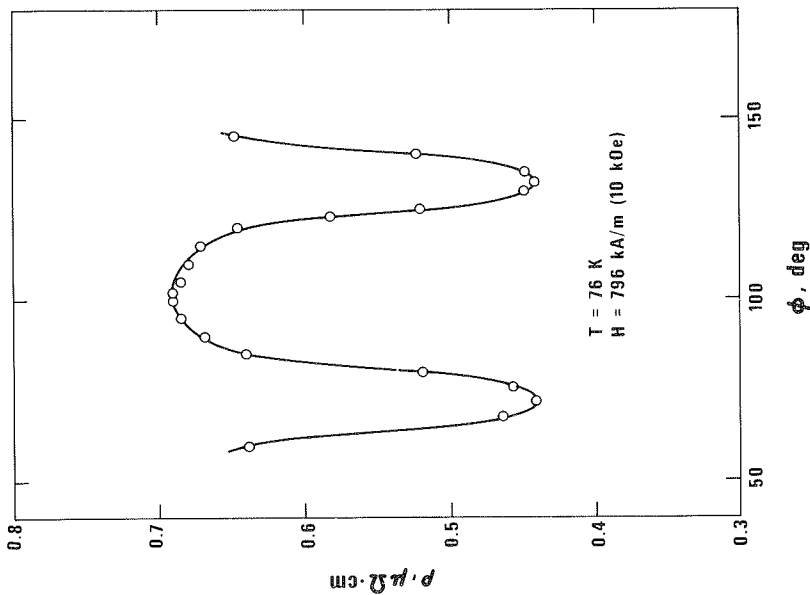


Fig. 4. The electrical resistivity of high-purity single-crystal beryllium at 76 K as a transverse magnetic field of 796 kA/m (10 kOe) is rotated about the basal plane. The angle  $\phi$  is an arbitrary angle.

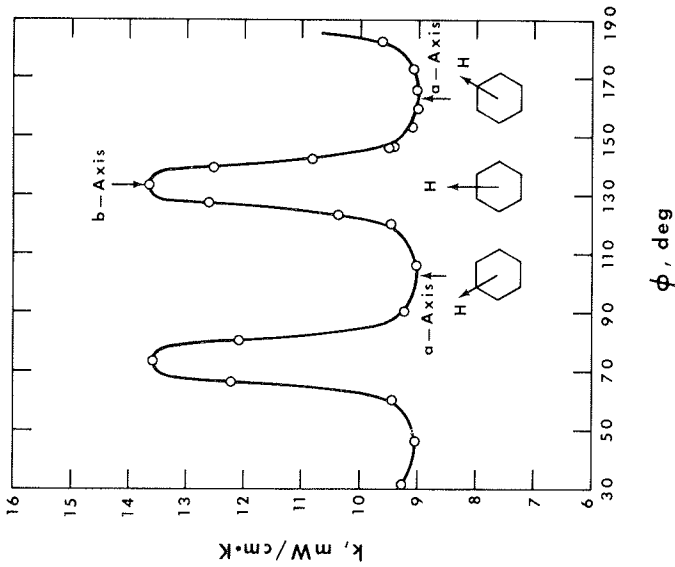


Fig. 6. The thermal conductivity of high-purity single-crystal beryllium at 2.1 K as a transverse magnetic field of 796 kA/m (10 kOe) is rotated about the basal plane. The angle  $\phi$  is an arbitrary angle.

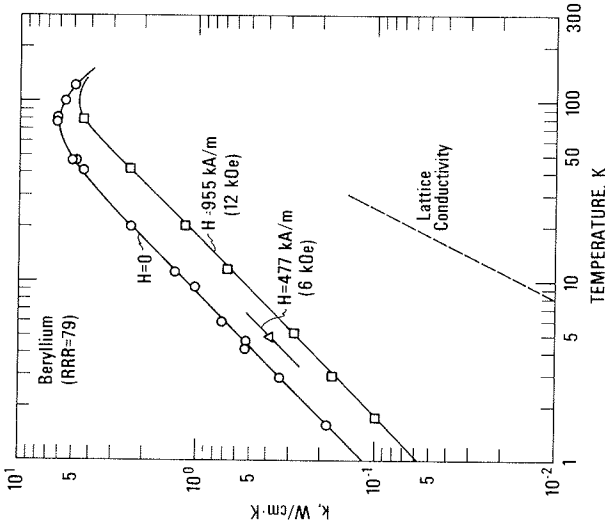


Fig. 7. The thermal conductivity of low-purity single-crystal beryllium as a function of temperature for various transverse magnetic fields. The lattice conductivity derived from the measurements on high-purity beryllium is shown for comparison.

hexagonal  $c$  axis  $[0001]$  and the transverse magnetic field was along one of the  $a$  axes  $\langle 11\bar{2}0 \rangle$  of the crystal. The dependence of thermal conductivity on the angle of the magnetic field in the basal plane is shown in Fig. 6 for a temperature of 4 K.

The thermal conductivity of the less pure sample 2 is shown in Fig. 7 as a function of temperature. The scatter of the zero-field data is much less than that for sample 1 because the thermal conductivity was lower and the indium solder provided better thermal contact to the reservoir than did the varnish used for sample 1.

## 4. DISCUSSION

### 4.1. Electronic and Lattice Thermal Conductivity

For  $H = 0$  and  $T < 150$  K the thermal conductivity of the high-purity sample is dominated by electron conduction. For that range the data are fit very well by the theoretically expected form

$$W_e = W_i + W_r = \alpha T^2 + \beta T^{-1} \quad (2)$$

where  $W_e$  is the total electronic thermal resistivity,  $W_i$  is the ideal resistivity due to phonon scattering, and  $W_r$  is the residual resistivity due to impurity scattering. The data of Fig. 5 give  $\alpha = (1.04 \pm 0.10) \times 10^{-5}$  cm/W K and  $\beta = 0.175 \pm 0.035$  cm K<sup>2</sup>/W. This was the first beryllium sample measured that was pure enough to allow a reliable determination of the ideal thermal resistivity. The uncertainties in  $\alpha$  and  $\beta$  stem from the difficulty in measuring the high conductivities with the low-conductance varnish joint. The quoted uncertainties represent the imprecision and also the inaccuracy of the data in zero field. In high magnetic fields the data imprecision decreases to about 1% but the inaccuracy (from geometrical uncertainties) is about 5%.

The thermal conductivity  $k$  has a contribution from the electrons  $k_e$  and from the lattice  $k_l$  such that  $k = k_e + k_l$ . The electronic thermal conductivity is so easily reduced by the application of a transverse magnetic field that the lattice thermal conductivity can contribute a sizable fraction to the overall conductivity in sufficiently high fields. The application of a magnetic field then allows a separation of the electronic and lattice components of conduction. Several methods exist for separating the two components from measurements in magnetic fields. In this work we use the method of Grüneisen and Adenstedt,<sup>5</sup> in which they write

$$k(H) = k_e(H) + k_l = L_e T \sigma(H) + k_l \quad (3)$$

where  $L_e$  is the electronic Lorenz number and  $\sigma(H)$  is the electrical conductivity in a magnetic field. In this expression  $L_e$  and  $k_l$  are assumed

independent of magnetic field. A plot of  $k(H)$  vs.  $T\sigma(H)$  for different field strengths yields a rather straight line for  $H > 150$  kA/m (2 kOe). Thus  $L_e$  and  $k_l$  are determined simultaneously. This technique was used at several temperatures to obtain the lattice conductivity shown in Fig. 5. For  $T < 30$  K, the lattice conductivity can be expressed as

$$k_l = \gamma T^2 \quad (4)$$

where  $\gamma = (1.6 \pm 0.2) \times 10^{-4}$  W/cm K<sup>3</sup>. Powell *et al.*<sup>14</sup> and White and Woods<sup>15</sup> estimated  $\gamma = 2.0 \times 10^{-4}$  W/cm K<sup>3</sup> from thermal conductivity measurements of beryllium alloys. Grüneisen and Adenstedt<sup>5</sup> derived the value 0.1 W/cm K for the lattice conductivity at 23.5 K from their measurements of the magnetothermal conductivity. That value is in excellent agreement with our results. The value of  $\gamma$  is lower than that of any other metal and is to be expected because of the high Debye temperature of beryllium. The lattice thermal conductivity of a material is usually expressed as

$$1/k_l = W_l = DT^{-2} + ET^{-2} + PT \quad (5)$$

where  $D$ ,  $E$ , and  $P$  are constants related to phonon–dislocation scattering, phonon–electron scattering, and phonon–point defect scattering. For a metal the phonon–electron term dominates the thermal resistance,<sup>16</sup> which explains the good agreement between the lattice conductivity from this work and that from previous work,<sup>14,15</sup> where the dislocation density would have been much higher.

Klemens<sup>17</sup> has calculated the lattice thermal conductivity of a metal for the case where phonon–electron interactions limit the conduction and for a spherical Fermi surface. His expression for the case where electrons interact with transverse as well as longitudinal phonons is

$$k_l = 313\alpha^{-1}\theta^{-4}n_0^{-4/3}T^2 \quad (6)$$

where  $\alpha$  is the term appearing in Eq. (2) for the ideal electronic thermal resistivity,  $\theta$  is the Debye temperature, and  $n_0$  is the number of free electrons per atom. Assuming the Fermi surface is spherical and using the value  $n_0 = 2$  in Eq. (6), we obtain  $k_l = 2.48 \times 10^{-6}T^2$  W/cm K, where the value  $\theta = 1481$  K is taken from the specific heat data of Ahlers.<sup>18</sup> The experimental value of  $k_l$  is nearly two orders of magnitude higher. If the electrons interact only with longitudinal phonons, then the numerical coefficient in Eq. (6) takes on the even smaller value of 105.<sup>17</sup> The thermal conductivity would be reduced further when the appropriate  $\theta$  for longitudinal phonons is used. The apparent large disagreement between theory and experiment for  $k_l$  is a result of the Fermi surface of beryllium, which is far from spherical.<sup>19</sup> Measurements of the de Haas–van Alphen effect in

beryllium<sup>19</sup> yield an effective  $n_0$  of 0.01573. That value of  $n_0$  in Eq. (6) gives  $k_l = 1.59 \times 10^{-3} T^2$  W/cm K for electrons interacting with transverse and longitudinal phonons, and  $k_l = 1.78 \times 10^{-4} T^2$  W/cm K for electrons interacting only with longitudinal phonons. The appropriate  $\theta$  used for the longitudinal phonons was 1947 K, which was calculated from elastic constant measurements.<sup>20,21</sup> The experimental value of  $k_l = (1.6 \pm 0.2) \times 10^{-4} T^2$  W/cm K suggests that the electrons interact only with longitudinal phonons, because of the good agreement with the calculated value for that case.

#### 4.2. Magnetoresistivities

A transverse magnetic field normally increases the electrical resistivity of a metal. The relative magnetoresistivity  $\Delta\rho/\rho(0)$ , where  $\rho(0)$  is the resistivity in zero field, may be plotted as a function of  $H\rho_\theta/\rho(0)$ , where  $\rho_\theta$  is the resistivity at the Debye temperature. This type of plot is known as the reduced Kohler diagram.<sup>1</sup> For a given crystallographic direction one curve in the reduced Kohler diagram should fit data taken at any temperature and with any impurity level. Figure 8 is the reduced Kohler diagram for beryllium, which is based on data taken on sample 1 at three different temperatures. For this plot the value  $\rho_\theta = 47 \mu\Omega\text{-cm}$  at  $\theta = 1481$  K is estimated from the work of Powell.<sup>9</sup> As Fig. 8 shows, the magnetoresistance depends on the direction of the magnetic field. However, for both field directions the magnetoresistance has the  $H^2$  behavior at high fields that is theoretically predicted for a compensated metal with no open orbits. For  $H\parallel a$  the relative magnetoresistivity at high fields is given by  $\Delta\rho/\rho(0) = \xi[H\rho_\theta/\rho(0)]^2$  with  $\xi = 1.45 \times 10^{-17} \text{ m}^2/\text{A}^2$ . For  $H\parallel b$  the coefficient is  $\xi = 8.9 \times 10^{-18} \text{ m}^2/\text{A}^2$ . Previously published results<sup>1,22</sup> for the case of  $H\parallel a$  give the value  $\xi = 3.5 \times 10^{-17} \text{ m}^2/\text{A}^2$ . The lower value found here is due entirely to the use of a higher  $\theta$  to evaluate  $\rho_\theta$ .

The electronic thermal resistivity in a magnetic field can be written as

$$W_e(H) = \rho(H)/L_e T \quad (7)$$

Because  $L_e$  is independent of magnetic field, the change of  $W_e$  with field should be proportional to that of  $\rho$ . Thus  $\Delta W_e/W_e(0)$  should be equal to  $\Delta\rho/\rho(0)$ . Figure 9 is the reduced Kohler plot for the electronic thermal resistivity at 4 K. For high fields  $\Delta W_e/W_e(0)$  is proportional to  $[H\rho_\theta/\rho(0)]^2$  with a proportionality constant of  $1.2 \times 10^{-17} \text{ m}^2/\text{A}^2$ . The dashed line in Fig. 9 is the curve for  $\Delta\rho/\rho(0)$ . The difference between  $\Delta\rho/\rho(0)$  and  $\Delta W_e/W_e(0)$  is probably within experimental error. The uncertainty in  $W_e(0)$  is as high as 25% because of the difficulty in measuring such a low thermal resistance. If  $\Delta W_e/W_e(0)$  were forced to agree with the  $\Delta\rho/\rho(0)$  curve (the more accurate

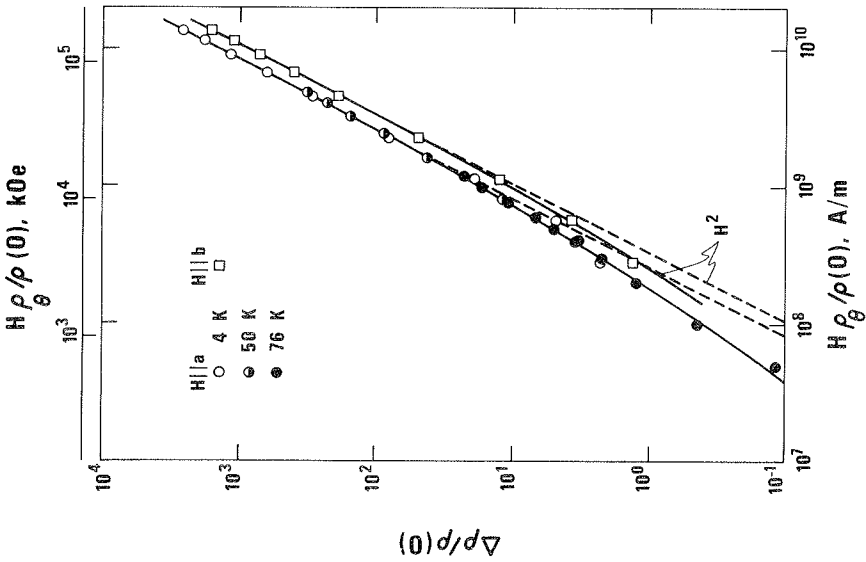


Fig. 8. A reduced Kohler plot of the electrical magnetoresistivity of high-purity single-crystal beryllium for two directions of the magnetic field and three different temperatures.

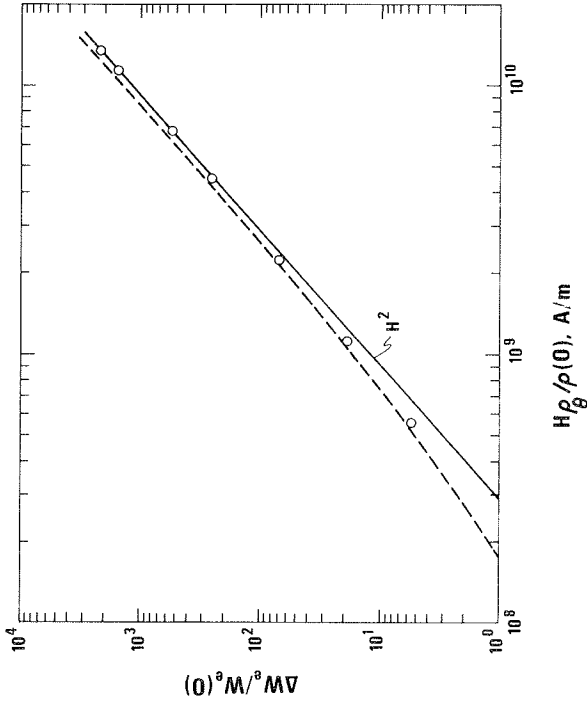


Fig. 9. A reduced Kohler plot of the thermal magnetoresistivity of high-purity single-crystal beryllium at 4 K with the magnetic field along the *a* axis. The solid line is proportional to  $H^2$  and is a fit to the high-field data. The dashed line represents the curve for  $\Delta\rho/\rho(0)$  with the same field direction.

of the two), then the zero-field thermal resistivity would be decreased such that  $\beta$  in Eq. (2) would be  $0.145 \text{ cm K}^2/\text{W}$  instead of  $0.175$ .

### 4.3. Lorenz Ratio

The Lorenz ratio is defined as

$$L = \rho k / T \quad (8)$$

For the elastic impurity scattering region at low temperatures and for temperatures well above the Debye temperature, the Lorenz ratio should approach the universal value  $L_0 = 2.44 \times 10^{-8} \Omega \text{ W}/\text{K}^2$ . Figure 10 shows the temperature dependence of  $L/L_0$  for beryllium sample 1. The dashed lines represent the extreme values from measurement uncertainties. The high-temperature end of the curve blends in well with the high-temperature data of Powell.<sup>9</sup> The low-temperature behavior for  $L/L_0$  does not approach 1 as expected for impurity scattering. It should be noted, however, that a value of 1 is within the experimental uncertainty. It was found in the previous section that a thermal resistivity value  $W_r = 0.145 \text{ T}^{-1} \text{ cm K}/\text{W}$  gave consistent

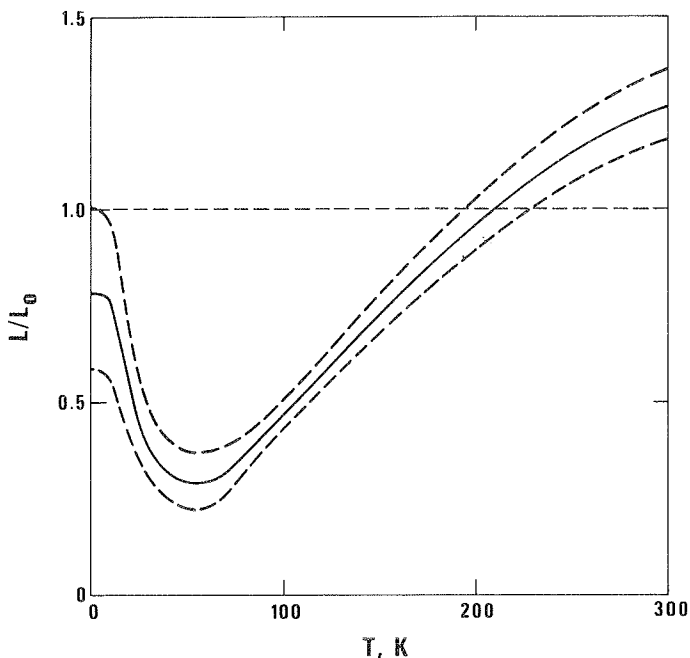


Fig. 10. The Lorenz ratio  $L = \rho k / T$ , reduced by the universal value  $L_0 = 2.44 \times 10^{-8} \Omega \text{ W}/\text{K}^2$ , as a function of temperature for high-purity single-crystal beryllium.

results for the magnetoresistivity in the thermal and electrical cases. That thermal resistivity value would then give  $L/L_0 = 0.95$  at  $T = 0$ . The value of  $L_e$  determined from Eq. (3) also gives  $L_e/L_0 = 0.95$  for temperatures below 10 K.

#### 4.4. Heat Switch

For temperatures below about 30 K, the thermal conductivity of beryllium sample 1 could be changed by over three orders of magnitude with a magnetic field of 955 kA/m (12 kOe). That is roughly equivalent to a change in thermal conductivity from that of high-purity copper to that of stainless steel. Thus beryllium would be a useful heat switch for temperatures up to about 30 K. This upper temperature limit is higher than for any other metal. For example, gallium and tungsten could only be used up to about 10 K. The fabrication of a heat switch of beryllium must be done with the proper precautions so as not to allow toxic dust particles of beryllium to escape to the atmosphere. A comparison of the results on samples 1 and 2 shows that a resistance ratio greater than about 1000 is needed for a good beryllium heat switch.

#### ACKNOWLEDGMENTS

I wish to thank Dr. R. J. Soulen and Dr. S. K. Sinha for supplying the samples used in this work. The assistance of Dr. H. M. Ledbetter and Mr. R. E. Schramm on the x-ray analysis is gratefully acknowledged. I also want to thank Dr. J. D. Siegwarth for constructing part of the apparatus and for many valuable discussions.

#### REFERENCES

1. G. T. Meaden, *Electrical Resistance of Metals* (Plenum Press, New York, 1965), p. 133.
2. J. M. L. Engels, F. W. Gorter, and A. R. Miedema, *Cryogenics* **12**, 141 (1972).
3. W. J. DeHaas and J. DeNobel, *Physica* **4**, 449 (1938); J. DeNobel, *Physica* **23**, 261 (1957).
4. J. R. Long, *Phys. Rev. B* **3**, 1197 (1971).
5. E. Grüneisen and H. Adenstadt, *Ann. Physik* [5] **31**, 714 (1938).
6. E. Grüneisen and H. D. Erfling, *Ann. Physik* [5] **38**, 399 (1940).
7. H. D. Erfling and E. Grüneisen, *Ann. Physik* [5] **41**, 89 (1942).
8. E. J. Lewis, *Phys. Rev.* **34**, 1575 (1929).
9. R. W. Powell, *Phil. Mag.* **44**, 645 (1953).
10. W. N. Lawless, *Rev. Sci. Instr.* **42**, 561 (1971).
11. L. J. Neuringer and Y. Shapira, *Rev. Sci. Instr.* **40**, 1314 (1969).
12. L. L. Sparks and R. L. Powell, *J. Res. NBS* **76A**, 263 (1972).
13. R. Reich, V. Q. Kink, and J. Bonmarin, *C. R. Acad. Sci. Paris* **256**, 5558 (1963).
14. R. L. Powell, J. L. Harden, and E. F. Gibson, *J. Appl. Phys.* **31**, 1221 (1960).
15. G. K. White and S. B. Woods, *Can. J. Phys.* **33**, 58 (1955).

16. H. M. Rosenberg, *Low Temperature Solid State Physics* (Oxford University Press, London, 1963), p. 120.
17. P. G. Klemens, *Aust. J. Phys.* **7**, 57 (1954).
18. G. Ahlers, *Phys. Rev.* **145**, 419 (1966).
19. J. H. Tripp, R. M. Everett, W. L. Gordon, and R. W. Stark, *Phys. Rev.* **180**, 669 (1969).
20. J. F. Smith and C. L. Arbogast, *J. Appl. Phys.* **31**, 99 (1960).
21. G. Simmons and H. Wang, *Single Crystal Elastic Constants and Calculated Aggregate Properties: A Handbook*, 2nd ed., (MIT Press, Cambridge, Massachusetts, 1971).
22. G. Aschermann and E. Justi, *Phys. Z.* **43**, 207 (1942).

